AN ELASTIC-PLASTIC FRACTURE INVESTIGATION ON STABLE CRACK GROWTH FOR PLANE STRESS

Xu Jilin (徐纪林) Xue Yinian (薛以年) Han Jinhu (韩金虎)
Institute of Mechanics, Academia Sinica, China

ABSTRACT

In this paper the stable crack growth processes in aluminium alloy sheet specimens with flat or inclined central crack, subjected to uniform tensile load have been investigated. The relations between the tensile load and the amount of crack extension were obtained. The deformation field was measured by using laser speckle method and moiré method. The finite element analysis based on large elastic-plastic deformation equation has also been carried out. The criterion proposed to predict cract growth under mode I condition is that the tensile strain at the crack tip reaches the maximum elongation of the material. The calculated results are in good agreement with the experimental data.

INTRODUCTION

For ductile material under plane stress condition the extensive plastic zone occurs before the initiation of crack growth. The application of LEFM to this situation usually underestimates the structure strength. In recent years several elastic-plastic fracture criteria were proposed. Based on each of these criteria the fracture parameters as well as the strain field around the crack tip in the case of large scale yielding were calculated by using finite element method[1][2]. Little has been investigated on the mixed mode fracture under large scale yielding condition. Ueda[3] studied the mixed mode brittle fracture initiation under large scale yielding.

In this paper the stable crack growth processes under mode I and

mixed mode have been investigated by experiments and finite element analysis. The calculated results are compared with the experimental data.

EXPERIMENT

Tests were conducted on LY12-CZ and LY12-CS aluminium alloy sheet specimens under uniaxial tension, containing a central crack which was inclined to the load line with angles β=90°, 60°, 45°, 30° (Fig. 1). The mechanical properties are given in Table 1. The total crack length ranged

Table 1

Material	Young's Modulus	Yielding Strength	Ultimate Strength	Maximum Elongation
	$E(kg/mm^2)$	$\sigma_{ys}(kg/mm^2)$	$\sigma_u(kg/mm^2)$	ε_f
LY12-CZ	7100	32.5	45.5	0.184
LY12-CS	7100	32.5	45.2	0.143

from 4.65 mm to 42.7 mm. Most of the specimens were fatigue-precracked with five of them not fatigue-precracked for the purpose of comparison.

The amount of crack extension was measured by microscope with magnification ratio of 80. The deformation field was obtained by using laser speckle method on one surface of a specimen and moiré method on the other surface[4]. In the whole-field analysis, the measuring sensitivity of the laser speckle direct record method is equivalent to that of moiré method with 467 line/mm density. Thus, the laser speckle method was used to measure the deformation field for lower loading while the convenient moiré method with 40 line/mm density of orthogonal grating was used for higher loading.

FINITE ELEMENT ANALYSIS

An Eulerian finite element formulation for large elastic-plastic deformation[5] was used. The finite element mesh used for specimens with inclined central crack is shown in Fig. 2(a). For β=90°, due to symmetry, only a quarter of the specimen was analyzed as shown in Fig. 2(b). The ratio of the element size at the crack tip to the crack length ranged from 1/40 to 1/100.

For specimens with β=90°, based on the strip necking zone model[6],

the crack tip opening displacements were calculated by finite element method. The width of the strip necking zone was taken equal to the thickness of the sheet. The tensile strain at the crack tip ε_δ was defined as the ratio of the CTOD to the sheet thickness (ε_δ = CTOD/t)[7]. The criterion used to predict crack growth is that the tensile strain at the crack tip reaches the maximum elongation of the material. The crack growth was simulated in the following way. As the crack tip advances to the next node the restraining force at the crack tip is gradually relaxed to zero in five equal steps. The relations between the tensile load and the amount of the crack extension were obtained.

The calculation was also carried out on the specimens with (β=60°, 45°, 30°) using the large elastic-plastic deformation equations. The stress and strain field as well as the plastic region configuration were obtained. The calculated results are compared with the experimental data.

RESULTS AND DISCUSSION

(1) Fracture Appearance It can be seen that for all the specimens full shear lips are developed after a very short transition of flat fracture from the crack tip. Thus the plane stress condition was met.

(2) Fracture Stress The applied stress and the average stress on ligament at crack initiation, σ_i and σ_i(net), as well as σ_c and σ_c (net) at fracture obtained from experiment are listed in Table 2 in normalized form. The ratios of σ_i(net) to yield strength σ_{ys} are nearly one. It shows that the specimens underwent large plastic deformation before the initiation of crack growth.

The applied stresses σ_i and σ_c increase with W/b. They do not vary with β if the ratios W/b are approximately the same. The fracture stresses σ_c are essentially independent of the sheet thickness under the plane stress condition.

(3) Fatigue Precrack As shown in Table 2, if the specimens were not fatigue-precracked, the tensile stress at initiation σ_i is approximately equal to the fracture stress, σ_c. However, if the specimens were fatigue-precracked, σ_c is evidently higher than σ_i. And in the fracture process the former exhibited less stable crack growth than the fatigue-precracked specimen.

(4) Crack Growth Process The relations between applied stress, σ and the amount of crack extension, $a-a_0$ were obtained from the experiment as

No.	β	t (mm)	$2a_0$ (mm)	$2\bar{a}_0$ (mm)	$\frac{W}{b}$	$\frac{\sigma_i}{\sigma_{ys}}$	$\frac{\sigma_c}{\sigma_{ys}}$	$\frac{\sigma_{i(net)}}{\sigma_{ys}}$	$\frac{\sigma_{c(net)}}{\sigma_{ys}}$
1	90°	0.45	11.79	11.79	0.891	0.914	0.972	1.025	1.129
2		0.45	12.36	12.36	0.885	0.855	0.945	0.963	1.029
3		0.45	12.62	12.62	0.883	0.809	0.945	0.917	1.095
						(0.943)	(0.987)		
4*		0.45	11.05	11.05	0.898	0.963	0.982	1.077	
5		0.89	4.65	4.65	0.957	1.071	1.095	1.117	1.175
6		0.89	5.81	5.81	0.946	1.031	1.086	1.092	1.175
7		0.89	11.55	11.55	0.893	0.899	1.003	1.009	1.166
						(0.958)	(1.005)		
8		0.89	18.30	18.30	0.830	0.720	0.889	0.868	1.132
9		0.89	23.78	23.78	0.780	0.720	0.831	0.926	1.111
10*		0.89	10.10	10.10	0.906	0.939	0.954	1.034	
11	60°	0.91	23.41	20.27	0.812	0.705	0.886	0.868	1.092
12		0.91	23.69	20.52	0.810	0.775	0.877	0.960	1.083
13*		0.91	23.67	20.50	0.810	0.868	0.889	1.071	1.098
14*		0.91	20.16	17.46	0.838	0.871	0.917	1.037	1.092
15**		1.50	22.10	19.14	0.823	0.825	0.908	1.000	1.102
16**		1.50	21.80	18.88	0.825	0.797	0.920	0.963	1.111
17		0.91	11.28	9.77	0.909	0.917	1.003	1.006	1.105
18		0.91	11.61	10.05	0.907	0.917	0.997	0.988	1.074
19	45°	0.91	30.13	21.30	0.803	0.751	0.871	0.939	1.086
20		0.91	30.21	21.36	0.802	0.751	0.871	0.939	1.086
21		0.91	30.79	21.77	0.798	0.763	0.865	0.957	1.083
22	30°	0.91	41.70	20.85	0.807	0.742	0.840	0.920	1.040
23		0.91	42.12	21.06	0.805	0.751	0.859	0.935	1.065
24		0.91	42.66	21.33	0.802	0.751	0.840	0.939	1.046
25*		0.91	40.20	20.10	0.814	0.880	0.892	1.083	1.098

$2\bar{a}_0 = 2a_0\sin\beta$, Material LY12-CZ, 2b=107.9mm, ( ) Calculated value

* Specimen not fatigue-precracked

** Material LY12-CS, 2b=110.0 mm

shown in Fig. 3(a). For mode I condition (β=90°), this relation obtained from the finite element method is shown in Fig. 3(b), which agrees fairly well with the experimental result. The applied stress at initiation from

calculation was somewhat higher than that in the experiment. In finite element analysis, the free crack surface had to extend one element ahead for each step of crack growth. This element mesh size was longer than the real amount of crack growth. As crack initiated in the test, the tensile strain at the crack tip attained only about two-thirds of the maximum elongation of the material, ε_f. Owing to these effects the applied stress at initiation were overestimated in calculation.

(5) Direction of Crack Extension During the crack growth in tests, all of the directions of crack extension for the specimens with inclined central crack of different β angles were essentially perpendicular to the load line as showin in Fig. 4. For all specimens the angles between the direction of crack extension and the X axis were less than 10°

The circumferential stress σ_θ distribution around the crack tip from calculation are shown in Fig. 4. The maximum value $\sigma_{\theta max}$ occurs in the element of β_E=90°, thus the direction of $\sigma_{\theta max}$ is parallel to the load line.

The relative displacement between the two crack surfaces at the nearest node about 0.4 mm from the crack tip, was regarded as the crack tip opening displacement $\overrightarrow{CODr}$ in the finite element analysis. The direction of $\overrightarrow{CODr}$ was approximately the same as that of the load line. For β=60°, 45° 30° angles between these two directions were about 4° to 10°

It can be seen that the predicted direction of crack extension from calculation was essentially identical with the experimental results.

(6) Plastic Zone The plastic zone calculated by finite element method is shown in Fig. 5. The shapes of the plastic zone for various inclined crack (β=60°, 45°, 30°) are similar. The lengths of plastic zone in x direction, X_p, obtained from calculation are approximately the same as that from experiment.

(7) Strain Field The strains in Y direction in ligament, ε_y are given in Fig.6(a), (b). The experimental data are slightly lower than the calculated results because the former are the average measured values at the distance between two isothetic fringes, this distance is larger than the element size.

The results of the calculation and the experiment show that the strains in X direction, ε_x are much smaller than ε_y. The shear strains γ_{xy} are also much smaller than ε_y in the calculation. Consequently, the strain in ligament is mainly determined by ε_y.

FINAL REMARKS

1. The proposed criterion for stable crack growth in plane stress condition is that the tensile strain at the crack tip reaches the maximum elongation of the material. Using this criterion in mode I condition, the calculated results agree well with the experimental data.

2. The fracture stresses are dominantly dependent upon the ratios of ligament length to sheet width, W/b for inclined central crack. That is to say, the fracture stress depends on the projections of the crack lengths in the direction perpendicular to the load line. And the fracture stress is essentially independent of the specimens thickness in plane stress condition.

3. During the stable crack growth process, the directions of crack extension for the specimens with inclined central crack are essentially prependicular to the load line. The strain field on ligament is mainly determined by ε_y. These show that it is possible to use the similar elastic-plastic fracture model and the above mentioned crack growth criterion of mode I to solve the mixed mode elastic-plastic fracture problem in plane stress condition.

REFERENCES

[1] Landes, J.D., Begley, J.A. and Clarke, G.A., Elastic-Plastic Fracture, ASTM STP 668, American Society for Testing and Materials (1979).

[2] Varanasi, S.R., in Flaw Growth and Fracture, ASTM STP 631 (1977), 507–519.

[3] Ueda, Y., Ikeda, K., Yao, T., Aoke, M., Shibasaki, S. and Shirakura, T., in Advances in Fracture Research, ICF5, Vol. 5 (1981), 2321–2328.

[4] Xue Yinian and Han Jinhu, Acta Mechanica Sinica, (5) (1981), 501–506.

[5] McMeeking, R.M. and Rice, J.R., Int. J. Solids Structures, 11 (1975), 601–616.

[6] Xu Jilin and Wang Ziqiang, in Advances in Fracture Research, ICF5, Vol. 4 (1981), 1697–1705.

[7] Xu Jilin, Acta Mechanica Sinica, (3) (1982), 272–279.

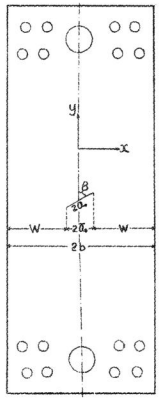

Fig.1 Specimen geometry

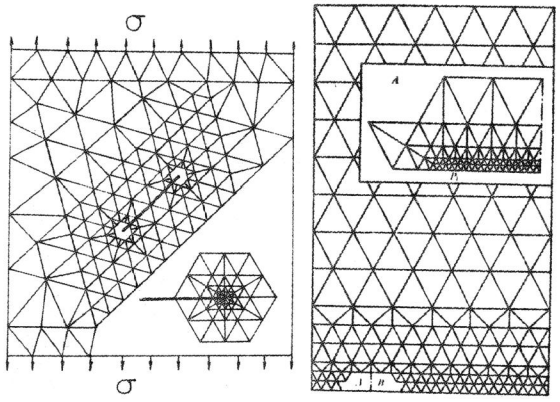

(a)β≠90° (b)β=90°
Fig.2 Finite-Element mesh

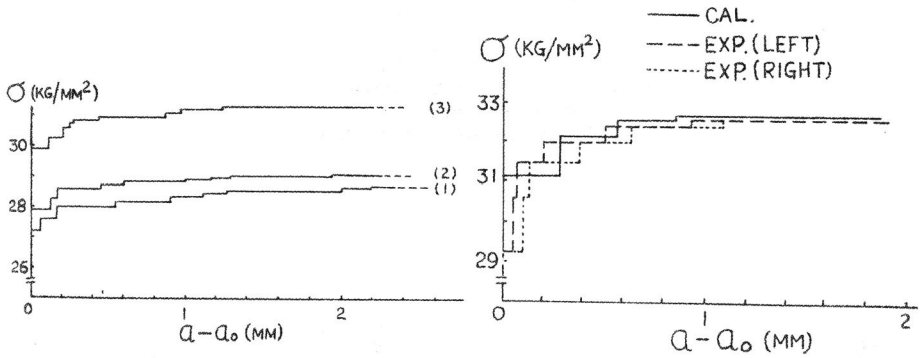

(1) (2) (3)
(a) β = 30° 45° 60°
Specimen No. 24 20 15

(b) specimen No.7, β=90°

Fig.3 Applied stress versus crack extension

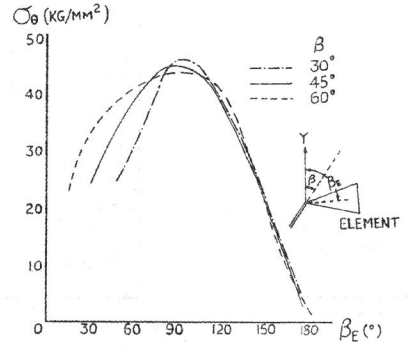

β = 60°, 45°, 30°
Fig.4 Specimens after fracture

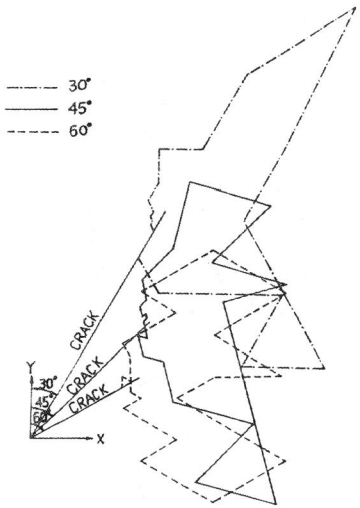

Fig.5 Circumferential stress around the crack tip (Specimen No. 15,20,24)

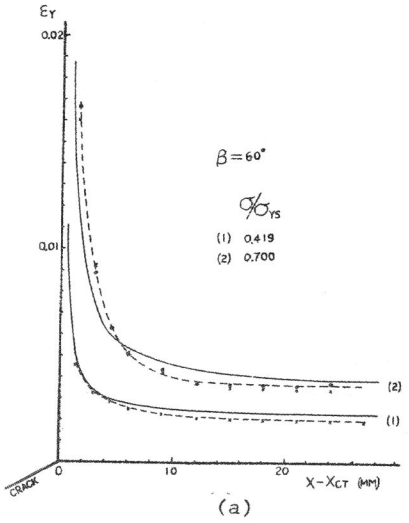

(a)

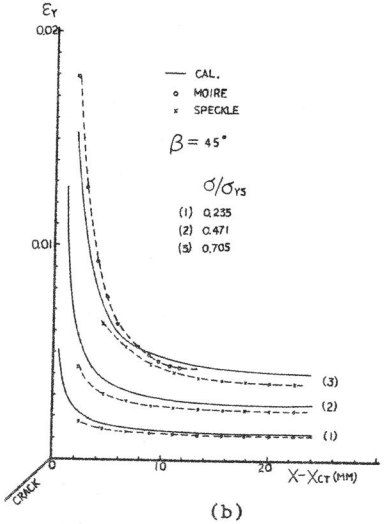

(b)

Fig.6 The strain in the ligament (a) Specimen No. 15 (b) Specimen No. 20